

***ragged seedling2* Encodes an ARGONAUTE7-Like Protein Required for Mediolateral Expansion, but Not Dorsiventrality, of Maize Leaves**

Ryan N. Douglas,^a Dan Wiley,^b Ananda Sarkar,^c Nathan Springer,^d Marja C.P. Timmermans,^c and Michael J. Scanlon^{a,1}

^aDepartment of Plant Biology, Cornell University, Ithaca, New York 14853

^bPlant Biology Department, University of Georgia, Athens, Georgia 30602

^cCold Spring Harbor Laboratory, Cold Spring Harbor, New York 11724

^dMicrobial and Plant Genomics Institute, Department of Plant Biology, University of Minnesota, Saint Paul, Minnesota 55108

Leaves arise from the flank of the shoot apical meristem and are asymmetrical along the adaxial/abaxial plane from inception. Mutations perturbing dorsiventral cell fate acquisition in a variety of species can result in unifacial (radially symmetrical) leaves lacking adaxial/abaxial polarity. However, mutations in maize (*Zea mays*) *ragged seedling2* (*rgd2*) condition cylindrical leaves that maintain dorsiventral polarity. Positional cloning reveals that *rgd2* encodes an ARGONAUTE7 (AGO7)-like protein required to produce ta-siARF, a *trans*-acting small interfering RNA that targets abaxially located *auxin response factor3a* (*arf3a*) transcripts for degradation. Previous studies implicated ta-siARF in dorsiventral patterning of monocot leaves. Here, we show that *arf3a* transcripts hyperaccumulate but remain abaxialized in *rgd2* mutant apices, revealing that ta-siARF function is not required for *arf3a* polarization. RGD2 also regulates miR390 accumulation and localization in maize shoot apices. Similar to the abaxialized maize mutant *leafbladeless1* (*lbl1*), *rgd2* mutants exhibit ectopic accumulation of the abaxial identity factor miR166 in adaxial domains. Thus, hyperaccumulation of *arf3a* and ectopic accumulation of miR166 are insufficient to condition abaxialized leaf phenotypes in maize. Finally, transcripts of a maize *ago1* paralog overaccumulate in *lbl1* but not in *rgd2* mutants, suggesting that upregulation of *ago1* combined with ectopic accumulation of miR166 contribute to abaxialized leaf formation in *lbl1*. We present a revised model for the role of small RNAs in dorsiventral patterning of maize leaves.

INTRODUCTION

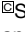
Shoot apical meristems (SAMs) are comprised of a group of indeterminate cells that give rise to all of the aboveground organs of the plant. The angiosperm SAM harbors stem cells that maintain the meristem by replacing cells lost during organogenesis. Leaves are initiated from the flank of the SAM in a position-dependent process whereby cells at the SAM periphery are recruited to become leaf founder cells (Poethig, 1984). As the founder cells are recruited and switch to determinate growth, leaf primordia are elaborated from the SAM along three main axes: the mediolateral axis (medial midrib to lateral margin), the proximodistal axis (proximal sheath to distal blade), and the dorsiventral axis (adaxial/abaxial). Maize (*Zea mays*) leaves are bifacial (dorsiventrally flattened) and harbor distinct tissue types on their adaxial (upper) and abaxial (lower) surfaces. By contrast, unifacial (radially symmetrical) leaf mutants are deficient in

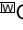
mediolateral development and typically lose either adaxial or abaxial epidermal patterning, with a concomitant conversion of the polarized vascular patterning seen in many wild-type plants (xylem is adaxial and phloem is abaxial) to an abaxialized mutant pattern (phloem surrounds xylem) or an adaxialized mutant vasculature (xylem surrounds phloem; Waites and Hudson, 1995; Timmermans et al., 1998; McConnell et al., 2001; Zhong and Ye, 2004; Eshed et al., 2004). Inspired by the snapdragon (*Antirrhinum majus*) unifacial leaf mutant *phantastica1*, a model for dorsiventral patterning was adapted to leaf development whereby the juxtaposition of adaxial and abaxial tissue types is required to organize the mediolateral and proximodistal axes of growth (Koch and Meinhardt, 1994; Waites and Hudson, 1995). Widespread support for this model is provided by phenotypic and molecular analyses of a number of unifacial leaf mutants from *Arabidopsis thaliana*, rice (*Oryza sativa*), tobacco (*Nicotiana benthamiana*), tomato (*Solanum lycopersicum*), and maize (*Zea mays*; reviewed in Kidner and Timmermans, 2007; Figure 1).

Unlike any previously described unifacial leaf mutants that are deficient in abaxial or adaxial patterning, the maize mutant *ragged seedling2* (*rgd2*) develops cylindrical leaves that maintain dorsiventral polarity (Henderson et al., 2005). Previous work has suggested that RGD2 function may be required to either interpret or respond to a proposed dorsiventral juxtaposition signal that initiates mediolateral development (Waites and Hudson, 1995; Henderson et al., 2005). Although the mechanisms whereby this

¹ Address correspondence to mjs298@cornell.edu.

The author responsible for distribution of materials integral to the findings presented in this article in accordance with the policy described in the Instructions for Authors (www.plantcell.org) is: Michael J. Scanlon (mjs298@cornell.edu).

 Some figures in this article are displayed in color online but in black and white in the print edition.

 Online version contains Web-only data.

www.plantcell.org/cgi/doi/10.1105/tpc.109.071613

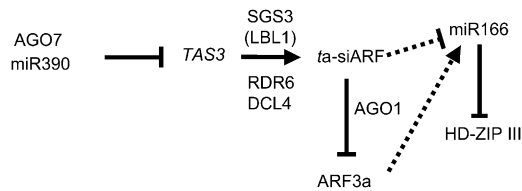


Figure 1. Proposed Model for the Role of Small Regulatory RNAs in Dorsiventral Patterning.

Model modified from Kidner and Timmermans (2007). Details provided in text. AGO7/RGD2, ARGONAUTE7/RAGGED SEEDLING2; miR390, microRNA 390; SGS3/LBL1, SUPPRESSOR-OF-GENE SILENCING3/LEAFBLADELESS1; RDR6, RNA-DEPENDANT RNA POLYMERASE6; DCL4, DICER-LIKE4; AGO1, ARGONAUTE1; ARF3a, AUXIN RESPONSE FACTOR3a; miR166, microRNA 166; HD-ZIP III, family of adaxial identity factors.

leaf patterning response is elaborated are still not fully understood, several microRNAs (miRNAs) and *trans*-acting small interfering RNAs (ta-siRNAs) are proposed to play important roles in establishing dorsiventral polarity in developing leaves (Figure 1; Nagasaki et al., 2007; Nogueira et al., 2007; reviewed in Husbands et al., 2009).

miRNA biogenesis requires DICER-LIKE1 function to process stem loop miRNA precursors into functional small RNAs (Reinhart et al., 2002). The processed miRNA combines with an ARGONAUTE (AGO) in an RNA-induced silencing complex (RISC) that can then target complementary mRNA sequences for silencing, either via cleavage of the target transcript or by translational inhibition (Fagard et al., 2000; Lanet et al., 2009). miR166 is required to spatially restrict the accumulation of adaxial-determining *class III homeodomain-leucine zipper (hd-zip III)* transcripts in both *Arabidopsis* and maize (McConnell et al., 2001; Juarez et al., 2004). Dominant mutations that disrupt the miR166 binding site of *hd-zip III* genes but preserve the protein coding sequence lead to unifacial leaf phenotypes wherein abaxial epidermal characteristics are lost (McConnell et al., 2001; Juarez et al., 2004).

The production of ta-siRNAs is a plant-specific process that uses components from both miRNA and small interfering (siRNA) biogenesis pathways. Biogenesis of ta-siRNAs begins with RISC-mediated cleavage of a non-protein-coding ta-siRNA precursor (*TAS*) transcript (Figure 1; Yoshikawa et al., 2005; Allen et al., 2005; Adenot et al., 2006; Fahlgren et al., 2006). Whereas the majority of small RNA-cleaved transcripts are summarily degraded, the *TAS* cleavage product is stabilized and processed into a double-stranded RNA. The formation of this double-stranded RNA requires SUPPRESSOR-OF-GENE SILENCING3 (SGS3) and RNA-DEPENDENT RNA POLYMERASE (RDR6; Allen et al., 2005; Nogueira et al., 2007). The resultant double-stranded RNA undergoes phased cleavage by DICER-LIKE4 (DCL4) to yield mature 21-nucleotide ta-siRNAs (Allen et al., 2005; Figure 1).

Four *TAS* gene families (*TAS1*, *TAS2*, *TAS3*, and *TAS4*) are found in *Arabidopsis*, whereas *tas3* is the only *tas* family described in maize to date (Nogueira et al., 2007). Posttranscriptional cleavage of *TAS3* precursor genes requires a specialized

RISC containing miR390 and AGO7/ZIPPY (ZIP). After post-transcriptional cleavage, SGS3-RDR6-DCL4 processes the *TAS3* cleavage product into 21-bp ta-siRNAs, a subset of which are called ta-siARFs (Peragine et al., 2004; Allen et al., 2005; Montgomery et al., 2008). As a small RNA substrate bound by AGO1 during posttranscriptional cleavage of the transcription factors *AUXIN RESPONSE FACTOR3/ETTIN (ARF3/ETT)* and *ARF4*, ta-siARF regulates vegetative phase change in *Arabidopsis* shoots (Allen et al., 2005; Hunter et al., 2006). Subsequently, ta-siARF was shown to function redundantly to regulate organ polarity, wherein *arf3/ett* and *arf4* are abaxial determinants (Pekker et al., 2005; Garcia et al., 2006; Fahlgren et al., 2006).

Genetic analyses in maize and rice have demonstrated a primary role for ta-siARF during dorsiventral leaf patterning; mutations in this ta-siRNA pathway generate shootless embryos or filamentous, abaxialized leaf phenotypes (Nagasaki et al., 2007; Nogueira et al., 2007, 2009). By contrast, *Arabidopsis* mutants in the *TAS3* ta-siRNA pathway show no defects in leaf polarity but render a precocious switch from juvenile to adult-staged leaves (Hunter et al., 2003; Peragine et al., 2004). *Leaf-bladeless1 (lbl1)* encodes the maize homolog of SGS3 (Nogueira et al., 2007). Macroscopically, *lbl1* and *rgd2* have very similar mutant phenotypes (Timmermans et al., 1998; Henderson et al., 2005). However, closer inspection reveals that whereas severe *lbl1* unifacial leaves lose adaxial epidermal characteristics, *rgd2* cylindrical leaves maintain dorsiventral polarity. Recessive alleles of *lbl1* exhibit reduced levels of ta-siARF biogenesis and elevated levels of *arf3a*, which are purported to promote miR166 accumulation and condition an abaxialized phenotype (Figure 1; Nogueira et al., 2007, 2009). Surprisingly, *rgd2 lbl1* double mutants have a synergistic shootless phenotype, suggesting that RGD2 and LBL1 operate in overlapping pathways, yet also perform some nonredundant functions (Henderson et al., 2006).

Here, we show that *rgd2* encodes a maize AGO7-like protein required for ta-siARF biogenesis and downregulation of *arf3a* transcripts. Surprisingly, *arf3a* transcript accumulation remains abaxialized in *rgd2* and *lbl1* mutants, revealing that ta-siARF function is not required for *arf3a* polarization. RGD2 function is also required for proper localization and downregulation of miR390 and miR166 in maize shoot apices. Combined with previous genetic and phenotypic analyses of the *rgd2-R* mutation, these data suggest that *arf3a* overaccumulation and ectopic accumulation of miR166 are insufficient to confer the loss of dorsiventral polarity in maize leaves. An *ago1* homolog hyperaccumulates in *lbl1-rgd1* but not in *rgd2-R* mutants. Taken together, these findings suggest that LBL1 regulates miR166 localization in a separate pathway that does not require RGD2 function, and the combined overaccumulation of *ago1* together with ectopic miR166 triggers abaxialized leaf phenotypes that are not observed in *rgd2* mutants.

RESULTS

Positional Cloning of *rgd2*

A mapping population of 189 highly introgressed individuals (see Methods) was used to genetically map the *rgd2-R* mutation to

within a 0.52-centimorgan interval on maize chromosomal bin 1.04. This interval is flanked by the markers IDP1473 and CAP276M21 and is comprised of ~1.2 megabase pairs on contig 19 of the maize genome (Figure 2A; see Supplemental Table 1 online; Maize Sequence Release 4a.53, October 2009). Among the 40 predicted genes within this interval, a maize homolog (GRMZM2G365589) of *Arabidopsis* AGO7/ZIP was investigated as a candidate *rgd2* gene.

The *rgd2-R* mutation arose in a *Mutator* (*Mu*) transposon-mutagenized background (Henderson et al., 2005); the *ago7* candidate gene was used as a probe in a DNA gel blot hybridization to search for a gene-specific *Mu* insertion in *rgd2-R* mutant plants. Compared with the inbred lines Mo17 and B73, *rgd2-R* mutants contained an ~1.6-kb insertion in the maize *ago7*-like gene (Figure 2B; see Supplemental Figure 1 online). Analyses of genomic PCR products obtained using an *ago7*-specific primer and a degenerate *Mu* transposon primer (*MuTIR*) revealed the presence of a *Mu5* (Talbert et al., 1989) transposon located 96 bp into the first intron of the *rgd2-R* allele of *ago7*. Attempts to span the *Mu5* insertion site using *ago7*-specific primers (F1 and R1) in RT-PCR of cDNA derived from *rgd2-R* mutants failed (Figure 2C), suggesting that the *Mu5* transposon is improperly spliced from *ago7* transcripts of *rgd2-R* mutants. RT-PCR analyses using an *ago7*-specific primer (F1) and the *MuTIR* primer yielded an aberrant *ago7* cDNA fragment in which the *Mu5* terminus was spliced directly into the first exon of *ago7*, indicating that *rgd2-R* is a null mutation.

Identification of three additional mutant alleles verified that *rgd2* is an *ago7*-like maize gene (Figure 2B). Two alleles were obtained via ethyl methanesulfonate (EMS) mutagenesis; *rgd2-e1* conditions a severe phenotype and contains a canonical G-to-A transition at the last base pair of the second intron. A predicted null allele, *rgd2-e1*, produces a mis-spliced transcript containing a premature stop codon that is predicted to eliminate the conserved PIWI domain of RGD2 (described below). A second EMS allele with a relatively mild ragged seedling phenotype, *rgd2-e2*, contains a G-to-A transition in the third exon that is predicted to cause a Gly to Asp missense substitution at amino acid 612 (Figure 2B). A third mutant allele, *rgd2-Ds1*, contains a ~1.5-kb *Dissociation* (*Ds*) transposon insertion at base pair 3635 of the third exon. In the W22 inbred genetic background wherein *rgd2-Ds1* arose, plants homozygous for this allele are shootless (Figure 2B). Notably, the *rgd2-R* allele is also shootless when introgressed into W22. The independent origin of these four *rgd2* mutations, all of which contain lesions in the *ago7*-like locus (GRMZM2G365589), verifies that *rgd2* encodes an AGO7-like protein in maize.

Like its homologs in *Arabidopsis* (AGO7/ZIP) and rice (*SHOOT ORGANIZATION2/SHOOTLESS4* [*SHO2/SHL4*]), the *rgd2* locus contains three exons and is predicted to encode a protein of 1032 amino acids (Hunter et al., 2003; Nagasaki et al., 2007). RGD2 shares 61% identity/76% similarity with AGO7/ZIP and 76% identity/85% similarity with SHO2/SHL4 (see Supplemental Figure 2 online). RGD2 also contains the highly conserved PAZ domain (87.7% identity with SHO2 and 62.3% identity with AGO7) and the PIWI domain (86.6% identity with SHO2 and 69.0% identity with AGO7). PAZ domains are important for recognizing the 3' end of small RNAs, while PIWI domains

function during endonucleolytic slicing of target transcripts (reviewed in Vaucheret, 2008).

RGD2 Is Required for miR390 Localization

As an AGO7-like protein, RGD2 is predicted to regulate maize dorsiventral patterning via ta-siARF biogenesis (Figure 1; Nogueira et al., 2009). In situ hybridization of seedling apices revealed that *rgd2* transcript accumulation is not polarized (Figures 3A and 3B). Unlike the adaxial accumulation observed for AGO7 putative orthologs from *Arabidopsis* and rice (Itoh et al., 2008; Chitwood et al., 2009), *rgd2* transcripts are evenly accumulated throughout the adaxial and abaxial regions of the youngest leaf primordium (P0-P1) and accumulate weakly in the SAM. In older leaf primordia (P2-P6), transcripts are localized to the margins and vascular bundles. No transcript accumulation was detected using an *rgd2* sense control (Figure 3C).

Coimmunoprecipitation analyses in *Arabidopsis* showed that AGO7 selectively interacts with miR390 (Montgomery et al., 2008). Small RNA gel blot hybridizations were used to analyze the effect of the *rgd2-R* mutation on miR390 accumulation in maize shoot apices. As shown in Figure 4A, miR390 levels are significantly elevated in *rgd2-R* mutant apices compared with apices of wild-type seedlings. To determine if the *rgd2-R* mutation affects the tissue specificity of miR390 accumulation, locked nucleic acid (LNA) probes complementary to miR390 were used for in situ hybridizations of maize seedling shoot apices. As previously described and shown in Figures 3D and 3E, miR390 accumulates in adaxial domains of wild-type maize leaf primordia (Nogueira et al., 2009). By contrast, miR390 accumulation in the crown of the wild-type shoot apex is much lower than that observed in leaf primordia (Figure 3D). Polarized accumulation of miR390 is maintained in *rgd2-R* mutant leaf primordia; however, marked miR390 overaccumulation is observed in the crown of the *rgd2-R* mutant SAM compared with wild-type siblings (Figure 3F; see Supplemental Figure 3 online). By contrast, miR390 accumulation in the weakly phenotypic *rgd2-e2* mutant is similar to that observed in wild-type apices; very little miR390 is detected within the SAM crown (Figure 3G). An LNA probe complementary to murine miR124e was used as a negative control for all LNA in situ hybridizations; no signal is detected in maize tissues (Figure 3H).

RGD2 Is Required for ta-siARF Biogenesis and Regulation of *arf3a* Transcripts

AGO7 and miR390 are required to cleave the non-protein-coding *tas3* transcripts that serve as precursors to ta-siARFs, small RNAs that regulate *arf3a* transcript accumulation (Figure 1; Allen et al., 2005; Pekker et al., 2005; Hunter et al., 2006; Montgomery et al., 2008). While mature ta-siARF transcripts are shown to accumulate adaxially in maize leaf primordia (Nogueira et al., 2007), the accumulation pattern of the *tas3a* precursor has not been described. Transcripts of miRNA precursor genes are predicted to form a stem-loop secondary structure that prevents hybridization of probes complementary to the 21-bp miRNA sequence contained within the precursor RNA. Unlike miRNAs, however, the *tas3a* transcript is not predicted to form a

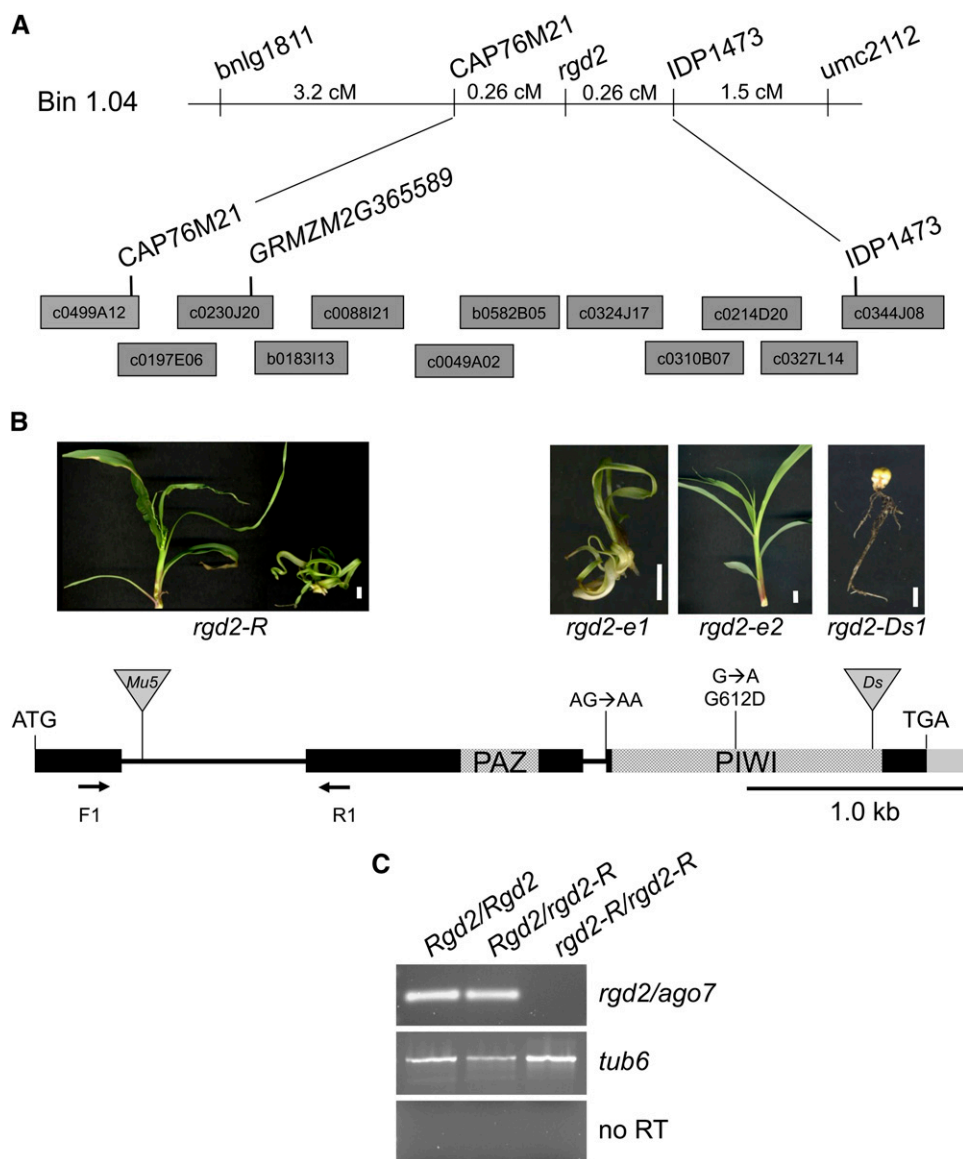


Figure 2. Positional Cloning and Characterization of *rgd2* Alleles.

(A) Positional cloning of *rgd2*. *rgd2-R* was mapped to bin 1.04 using simple sequence repeat markers (names) and fine mapped to an interval flanked by CAP76M21 and IDP1473. Candidate gene analysis revealed an *ago7*-like locus, GRMZM2G365589, on maize BAC c0230J20. Gray blocks indicate BAC clones. cM, centimorgan.

(B) Gene structure of *rgd2* wild-type and mutant alleles. The *rgd2* open reading frame consists of three exons (black boxes) and shows a high degree of similarity to *ago7*. Shaded boxes show the approximate positions of the predicted PAZ and PIWI protein domains. Solid gray box represents 3' untranslated region. Inverted triangles mark the locations of transposon insertions in the *rgd2-R* and *rgd2-Ds1* alleles. Point mutations in the EMS-induced alleles, *rgd2-e1* and *rgd2-e2*, are denoted. Images of representative phenotypes of *rgd2* mutant alleles are placed above each corresponding mutation. Bars = 1 cm.

(C) RT-PCR analysis of *rgd2* transcripts. Primers F1 and R1, which flank the first intron, were used in *rgd2* transcript analyses of seedlings from *rgd2-R* mutants, wild-type siblings, and heterozygous siblings. No transcripts were detected in *rgd2-R* mutants after 42 amplification cycles. RT-PCR using *tub6* primers served as the control. Three biological replicates comprising one seedling per replicate were performed.

[See online article for color version of this figure.]

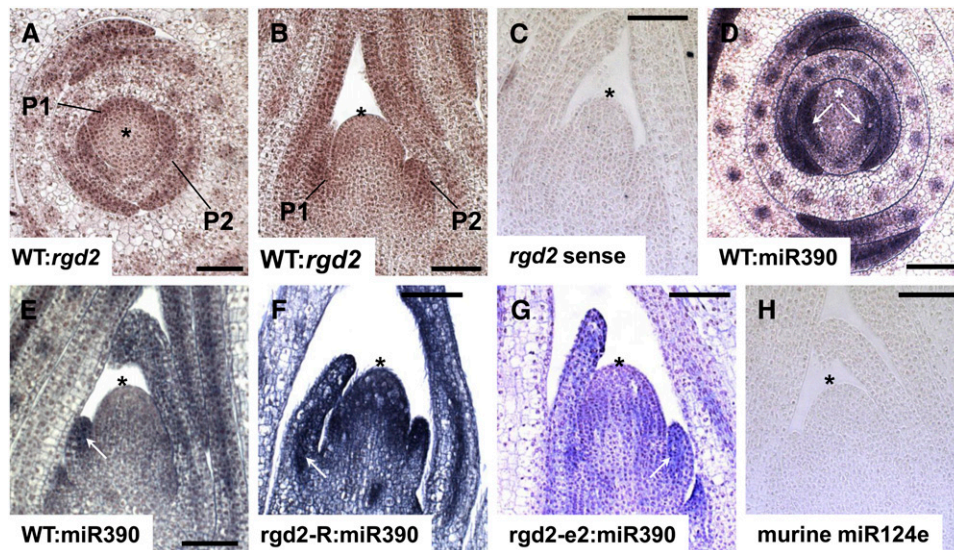


Figure 3. In Situ Hybridization Analysis of *rgd2* and miR390 Accumulation in *rgd2* Mutant and Wild-Type Sibling Apices.

(A) and (B) Accumulation pattern of *rgd2* in the SAM (asterisks) and leaf primordia (P1 and P2).

(A) Transverse wild-type shoot apex.

(B) Longitudinal wild-type shoot apex.

(C) Control in situ hybridization of wild-type shoot apex using a sense *rgd2* hybridization probe.

(D) to (G) Accumulation pattern of miR390.

(D) Transverse wild-type shoot apex.

(E) Longitudinal wild-type shoot apex.

(F) Longitudinal *rgd2*-R shoot apices show ectopic miR390 expression throughout the SAM crown and leaf primordia.

(G) Longitudinal *rgd2*-e2 shoot apex.

(H) An LNA probe for murine miR124e was used as a sense control for miR390 accumulation.

Bars = 100 μm; arrows indicate areas of transcript accumulation.

[See online article for color version of this figure.]

secondary structure that prevents the binding of a ta-siARF LNA probe to two complementary sites found within the *tas3a* mRNA (Nogueira et al., 2007). Thus, a probe complementary to ta-siARF is also expected to hybridize to *tas3a* precursor transcripts. As predicted, equivalent signals are detected in the abaxial regions of wild-type leaf primordia following in situ hybridization to either a *tas3a* antisense probe or to a 16-bp LNA probe that is complementary to the mature ta-siARF (Figures 5A to 5C). Previous studies revealed that precursor *tas3a* transcripts accumulate to much higher levels than mature ta-siARF (Allen et al., 2005; Lu et al., 2006). Taken together, these data suggest that the signal obtained following in situ hybridization of the ta-siARF LNA probe corresponds to *tas3a* precursor transcripts, which accumulate in abaxial leaf domains when RGD2 function is intact (Figures 5A to 5C). No accumulation is detected with a sense *tas3a* hybridization probe (Figure 5E). By contrast, the ta-siARF LNA probe identifies *tas3a* precursor transcripts in both adaxial and abaxial domains of *rgd2*-R leaf primordia, wherein RGD2 function is mutated (Figure 5D). These data suggest that *tas3a* transcripts initially accumulate throughout maize leaf primordia and are preferentially cleaved to generate ta-siARF in adaxial leaf domains by RGD2/miR390 activity, whereupon intact *tas3a* transcripts persist in abaxial regions.

Quantitative RT-PCR (qRT-PCR) confirmed that *tas3a* transcripts overaccumulate by 2.7-fold in *rgd2*-R mutant apices and by 7.9-fold in *rgd2*-R leaf primordia (P1-P4) compared with wild-type siblings (Figure 4B). Hyperaccumulation of *tas3a* transcripts in *rgd2*-R apices may reflect inefficient processing of *tas3a* precursors into ta-siARF in the mutant shoots. To test this hypothesis, the accumulation of ta-siARF in *rgd2*-R and wild-type apices was compared using small RNA gel blot hybridization. A 16-bp LNA probe complementary to ta-siARF detects a small RNA of the expected size in total RNA extracted from wild-type apices. By contrast, ta-siARF hybridization is dramatically reduced in RNA derived from *rgd2*-R mutant shoot apices (Figure 4A).

Proper biogenesis of ta-siARF is required to regulate *arf3a* accumulation in maize (Nogueira et al., 2007). Therefore, it was expected that *arf3a* transcripts would also be elevated in *rgd2*-R mutants owing to the absence of ta-siARF. Using cDNA prepared from laser microdissected (LM) SAM-P1 and leaf primordia (P1-P4) tissue, the accumulation of *arf3a* was examined by qRT-PCR. As expected, *arf3a* transcript accumulation is elevated in *rgd2*-R mutant SAMs (7.8-fold) and leaf primordia (35.9-fold) (Figure 4B) compared with the corresponding values in wild-type siblings.

Whereas *ARF3/ETT* transcripts accumulate throughout leaf primordia in *Arabidopsis*, accumulation of ARF3/ETT protein is

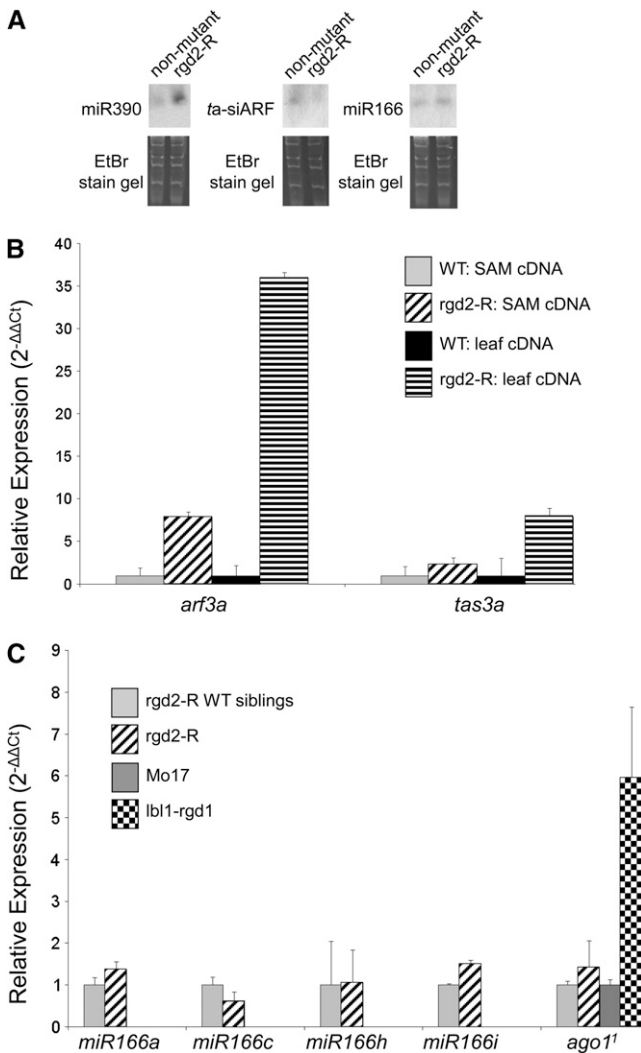


Figure 4. Accumulation Analyses of Transcripts Involved in the ta-siARF Pathway.

(A) Small RNA gel blot hybridization of miR390, miR166, and ta-siARF in wild-type and *rgd2-R* shoot apices. All genotypes are introgressed into the Mo17 genetic background.

(B) qRT-PCR analysis of *arf3a* and *tas3a* in laser-microdissected leaf primordia and SAMs from wild-type (WT) and *rgd2-R* mutants. Accumulation was normalized to *ubq*. Three biological replicates were performed per experiment. Error bars denote 1 SE.

(C) qRT-PCR analysis of miR166 precursors in laser-microdissected SAMs from wild-type and *rgd2-R* mutants. An *ago1* putative paralogue (¹GenBank accession number AY110984) was analyzed in wild-type, *rgd2-R* mutant, and *lbl1-ref* mutant 14-d-old seedlings. Accumulation was normalized to *tub6*. Each experiment used three biological replicates. Error bars denote 1 SE.

only detected in abaxial domains (Pekker et al., 2005; Chitwood et al., 2009). In situ hybridization analyses of wild-type shoot apices confirmed that *arf3a* transcripts in maize are preferentially abaxialized (Figure 5F), while no accumulation is detected using a sense *arf3a* probe (Figure 5I). Unexpectedly, *arf3a* transcript accumulation remains abaxialized in *rgd2-R* mutant leaves

(Figure 5G). An equivalent *arf3a* accumulation pattern was also observed in *lbl1-rgd1* mutants (Figure 5H), suggesting that ta-siARF biogenesis is not required to polarize *arf3a* accumulation within abaxial domains of maize leaf primordia.

RGD2 Regulates Abaxial Localization of miR166

Previous studies have suggested that miR166 accumulation is negatively regulated by ta-siARF and/or positively regulated by ARF3a (Figure 1; Nogueira et al., 2007, 2009). In light of these findings, the accumulation of *miR166* precursor loci was examined in *rgd2-R* mutant and wild-type SAM-P1 tissue by LM-qRT-PCR. Of the nine *miR166* precursor loci identified in the maize genome, four (*miR166a*, *miR166c*, *miR166h*, and *miR166i*) were previously shown to exhibit abnormal transcript accumulation in *lbl1* mutant shoots (Nogueira et al., 2007). However, the accumulation of these *miR166* precursor transcripts is not significantly increased in *rgd2-R* mutant apices compared with wild-type siblings (Figure 4C). By contrast, small RNA gel blot hybridization reveals that the 21-bp mature miR166 accumulates to approximately twofold higher levels in *rgd2-R* mutant apices (Figure 4A).

The tissue-specific accumulation of mature miR166 was examined by in situ hybridization using an LNA probe. In wild-type apices, miR166 accumulates in abaxial regions of young leaf primordia but is excluded from the SAM and from the pith directly below the SAM (Juarez et al., 2004; Figure 6A). Whereas *lbl1* mutants accumulate miR166 throughout the abaxial and adaxial domains of young leaf primordia and below the SAM (Juarez et al., 2004; Nogueira et al., 2007), *rgd2-R* mutants also exhibit ectopic miR166 accumulation in adaxial leaf domains but do not accumulate miR166 in the pith directly below the SAM (Figure 6B).

Recent studies have shown that SGS3 is required for siRNA-directed cleavage of *AGO1* transcripts in *Arabidopsis* (Mallory and Vaucheret, 2009). Using cDNA from 14-d-old maize seedlings, qRT-PCR was performed in *rgd2-R* and *lbl1-rgd1* mutant backgrounds. In congruence with *Arabidopsis*, a maize *ago1* putative paralog accumulates to nearly sixfold higher levels in *lbl1-rgd1* mutants than in the *rgd2-R* mutant or in wild-type plants (Figure 4C).

DISCUSSION

rgd2 Encodes AGO7 Function in Maize

rgd2-R is a recessively inherited mutant that is defective in mediolateral leaf development. Mutant plants often have cylindrical leaves that, unlike similar unifacial leaf mutants, maintain dorsiventral anatomy. No net loss of adaxial or abaxial characteristics is observed in *rgd2-R* mutant leaves (Henderson et al., 2005). The *rgd2* gene is identified as an *ago7*-like gene (GRMZM2G365589) using a positional cloning approach; several noncomplementing *ago7* mutant alleles were isolated to verify the identity of *rgd2* (Figures 2A and 2B). The *rgd2-R* reference allele harbors a *Mu5* transposable element within intron 1, and RT-PCR analyses of *rgd2-R* mutants fail to amplify

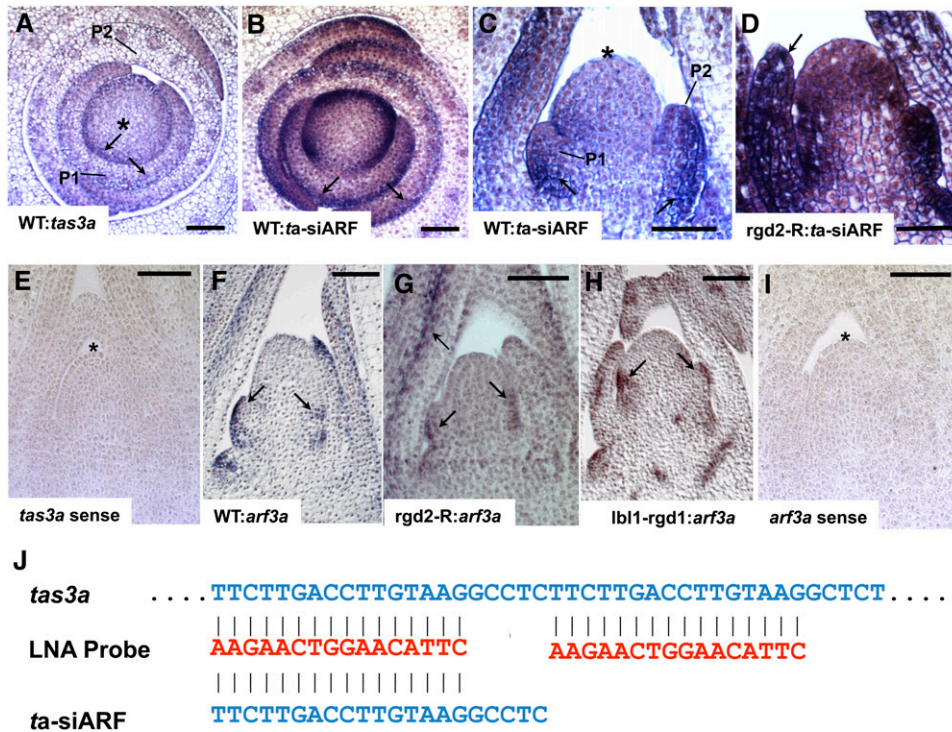


Figure 5. In Situ Hybridization Analysis of *tas3a* and *arf3a* in the Wild Type and in *rgd2-R* and *lbl1-rgd1* Mutants.

- (A) Accumulation of *tas3a* in a wild-type apex transverse section using a *tas3a* antisense hybridization probe.
 - (B) to (D) Pattern of transcript accumulation obtained using the ta-siARF LNA hybridization probe.
 - (B) Transverse section of a wild-type apex. Note that the pattern of transcript accumulation detected with the ta-siARF LNA probe is equivalent to that observed when using the *tas3a* probe (A).
 - (C) Longitudinal section of a wild-type SAM (asterisk) and leaf primordia (P1 and P2)
 - (D) Longitudinal section of a *rgd2-R* mutant apex shows ectopic transcript accumulation in the SAM and the leaf primordia.
 - (E) Control in situ hybridization of wild-type shoot apex using a sense *tas3a* hybridization probe.
 - (F) to (H) Accumulation pattern of *arf3a* transcripts.
 - (F) Longitudinal section of a wild-type apex reveals *arf3a* transcript accumulation in abaxial domains of leaf primordia.
 - (G) and (H) Longitudinal sections of *rgd2-R* (G) and *lbl1-rgd1* (H) mutant apices; *arf3a* transcript accumulation remains abaxialized in both.
 - (I) Control in situ hybridization of wild-type shoot apex using a sense *arf3a* hybridization probe.
 - (J) The LNA ta-siARF in situ hybridization probe is predicted to hybridize to the mature ta-siARF as well as to two locations in its abundant precursor, the *tas3a* transcript.
- Bars = 100 μm. Arrows point to areas of accumulation.
[See online article for color version of this figure.]

wild-type transcripts that span the exon 1–exon 2 boundary (Figure 2C). These data suggest that *rgd2-R* is a null allele. In *Arabidopsis*, AGO7 is implicated in the formation of ta-siARFs, which are required to downregulate the abaxial identity factors *ARF3* and *ARF4* (Allen et al., 2005; Pekker et al., 2005; Hunter et al., 2006). As predicted for a null allele of *ago7*, *rgd2-R* mutants are defective in ta-siARF biogenesis (Figure 4A) and show a concomitant increase in *arf3a* transcript accumulation (Figure 4B).

RGD2 Is Required to Localize miR390 in Maize Shoot Apices

Elegant and detailed coimmunoprecipitation analyses in *Arabidopsis* demonstrated that AGO7 forms a RISC exclusively with miR390 (Montgomery et al., 2008). Although the accumulation of

rgd2 and miR390 transcripts overlaps in young leaf primordia and developing vasculature, miR390 accumulates in adaxial domains (Nogueira et al., 2007; Figures 3D and 3E), whereas *rgd2* accumulation is apolar (Figures 3A and 3B). Adaxial accumulation of miR390 is maintained in *rgd2-R* mutant leaf primordia; however, marked overaccumulation of miR390 is observed within the crown of the mutant SAM (Figures 3F and 4A; see Supplemental Figure 3 online).

Layer-specific LM-qRT-PCR has shown that maize *mir390* precursor transcripts are expressed in the outer cell layer (L1) of the SAM but not in the L2 (Nogueira et al., 2009). Intriguingly, in situ hybridizations detect mature miR390 accumulation in both the L1 and L2 (Nogueira et al., 2009; Figure 3E). One possible explanation for this apparent discrepancy is that *mir390* precursor transcripts are processed more rapidly in the L2 than

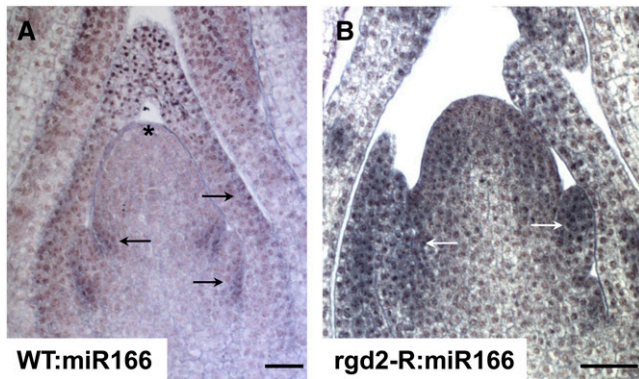


Figure 6. In Situ Hybridization Analysis of miR166 in the Wild Type and *rgd2-R* Mutants.

(A) and (B) Accumulation of miR166 in shoot apices. Bars = 50 μ m.
 (A) Longitudinal section of a wild-type apex shows miR166 accumulation in abaxial regions of leaf primordia (indicated by arrows). Asterisk denotes SAM.
 (B) Longitudinal section of an *rgd2-R* mutant apex shows ectopic accumulation of miR166 in adaxial regions of leaf primordia and the crown of the meristem (arrows).
 [See online article for color version of this figure.]

the L1; a second hypothesis is that mature miR390 is mobile and traffics from the L1 to the L2. Although ta-siRNAs are shown to act non-cell-autonomously (Chitwood et al., 2009), several studies examining the localization of artificial miRNAs and miRNAs with non-native promoters concluded that miRNAs act cell autonomously (Alvarez et al., 2006; Schwab et al., 2006; Tretter et al., 2008). Still other studies have suggested that miR166 and miR390 may traffic within the shoot apex (Juarez et al., 2004; Kidner and Martienssen, 2004; Nogueira et al., 2009). Our analyses of differential *rgd2* mutant alleles support a scenario wherein miR390 acts non-cell-autonomously, and RGD2 functions to restrict its mobility into the crown of the maize shoot apex.

The conserved PAZ domains of AGO proteins recognize and bind the 3' ends of small RNAs (Lingel et al., 2004; Ma et al., 2004; Hutvagner and Simard, 2008). The unspliced *Mu* insertion in *rgd2-R* mutant transcripts is expected to disrupt or eliminate the PAZ domain from RGD2, thereby preventing its binding of miR390, which overaccumulates ectopically in the *rgd2-R* mutant SAM crown (Figure 3F). By contrast, *rgd2-e2* mutants harbor a point mutation in the PIWI domain that causes a missense amino acid substitution; the PAZ domain is predicted to be unaltered (Figure 2B). Unlike *rgd2-R* mutants, *rgd2-e2* mutants do not show ectopic miR390 overaccumulation within the SAM crown (Figure 3G). Likewise, miR390 accumulation is unchanged in *lbl1* mutants (Nogueira et al., 2009), indicating that ta-siARF function is not required for proper localization of miR390. Taken together, these data suggest that an intact PAZ domain is correlated with normal miR390 accumulation in the maize SAM. We speculate that RGD2 is required to bind miR390 and restrict it from trafficking into the crown of the SAM (Figure 7).

Polarized Degradation of *tas3a* Is Patterned by Localization of miR390

An in situ hybridization probe that recognizes *tas3a* precursor transcripts was used to determine their accumulation pattern in wild-type shoot apices (Figure 5). Wild-type apices showed *tas3a* accumulation only in abaxial regions of leaf primordia, which is consistent with the biogenesis and function of ta-siARF in adaxial domains. An equivalent in situ hybridization signal is detected using a 16-bp LNA probe, which contains two complementary sites in the *tas3a* transcript (Figures 5B to 5D and 5J). In light of previous analyses revealing that ta-siARF accumulates to lower levels than most miRNAs (Allen et al., 2005; Lu et al., 2006), these data strongly suggest that the signals obtained with the ta-siARF LNA probe are derived from *tas3a* transcript accumulation and not ta-siARF accumulation.

Unlike wild-type siblings of *rgd2-R* mutants, ta-siARF LNA in situ hybridization analyses of *rgd2-R* mutants detect *tas3a* accumulation throughout the abaxial and adaxial domains of mutant leaf primordia (Figure 5D). These data suggest that the failure to process *tas3a* precursor transcripts into mature ta-siARF results in the ectopic accumulation of intact *tas3a* transcripts in *rgd2-R* mutant primordia. Both the overabundance of *tas3a* transcripts and the failure to detect ta-siARF in *rgd2* mutant shoots support this hypothesis (Figures 4A and 4B). AGO7 and miR390 are both required to cleave *tas3a* and begin the process of ta-siARF biogenesis (Montgomery et al., 2008). Although *rgd2* transcript accumulation is not polarized, miR390 is restricted to adaxial domains of maize leaf primordia (Figures 3A to 3D). These data indicate that the abaxial accumulation pattern of *tas3a* transcripts in wild-type leaves is patterned by the adaxial expression of miR390, not by RGD2 per se. By the same token, the ectopic *tas3a* accumulation observed in adaxial domains of

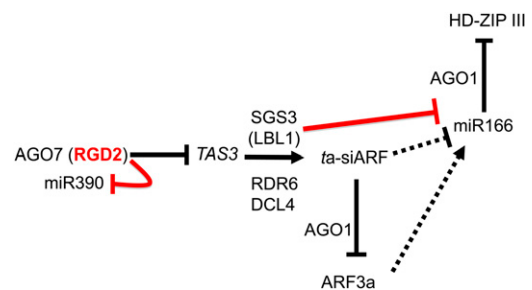


Figure 7. Revised Model for the Role of Small Regulatory RNAs in Dorsiventral Patterning.

rgd2 is the maize homolog of *Arabidopsis ago7* and is required to regulate miR390 accumulation and localization in the maize shoot apex. RGD2 and LBL1/SGS3 are both required to regulate miR166 accumulation levels. Like LBL1, RGD2 is required to properly localize miR166, suggesting that miR166 polarization requires ta-siARF function. Although *rgd2* mutants overaccumulate miR166 and *arf3a*, miR166 is properly localized, resulting in no net loss of dorsiventral patterning in *rgd2* mutants. However, in *lbl1* mutants, the ectopic accumulation of miR166 combined with the hyperaccumulation of *ago1* may account for the abaxialized mutant leaf phenotype. Abbreviations are as described in Figure 1.
 [See online article for color version of this figure.]

rgd2-R mutant leaf primordia is likely the result of failure to incorporate previously adaxialized miR390 into a functional RISC that normally converts *tas3a* into ta-siARF.

Upregulation of *arf3a* and Ectopic miR166 Are Insufficient to Confer an Abaxialized Leaf Phenotype in Maize

ARF3/ETT is an abaxial identity factor in *Arabidopsis* (Pekker et al., 2005); however, the absence of *arf3* mutants and/or ta-siARF insensitive lines has hindered analyses of ARF3 function in maize. *arf3a* transcript accumulation is detected in abaxial regions of wild-type maize (Figure 5F). Although the *rgd2-R* mutation confers marked overaccumulation of *arf3a* transcripts in the SAM and in young leaf primordia (Figure 4B), this accumulation pattern remains abaxialized (Figure 5G), and dorsiventral polarity is maintained in mutant cylindrical leaves (Henderson et al., 2005). A similar pattern of abaxialized *arf3a* transcript overaccumulation is observed in *lbl1 rgd1* double mutants, which are also defective in ta-siARF biogenesis (Figure 5H). Therefore, like the adaxialized expression of miR390, the abaxial accumulation of *arf3a* transcripts is regulated independently of ta-siARF biogenesis. Moreover, *rgd2-R* mutants retain dorsiventral leaf polarity (Henderson et al., 2005), suggesting that ta-siARF biogenesis is not a requirement for leaf polarity in maize.

Overexpression of a ta-siARF-insensitive *arf3/ett* transcript recapitulates the *zip-2/ago7* mutant phenotype in *Arabidopsis* (Hunter et al., 2006), which might suggest that the *rgd2-R* mutant phenotype is conditioned entirely by *arf3a* overaccumulation. However, mutations in putatively orthologous ta-siARF biogenesis genes condition disparate phenotypes in maize and *Arabidopsis* (Timmermans et al., 1998; Mourrain et al., 2000; Hunter et al., 2003; Peragine et al., 2004; Henderson et al., 2005), and in the absence of a maize ta-siARF insensitive line, this hypothesis remains quite speculative. On the other hand, the lack of abaxialized leaf phenotypes in *rgd2* mutants indicates that *arf3a* overaccumulation alone is not sufficient to disrupt dorsiventral leaf patterning in maize.

LBL1 encodes the maize SGS3 protein (Nogueira et al., 2007) and is thereby predicted to function directly downstream of RGD2 during ta-siARF biogenesis (Figure 1). Unlike *rgd2* mutants, however, *lbl1* mutations confer severe disruptions in dorsiventral patterning and abaxialized, unifacial leaf phenotypes (Timmermans et al., 1998; reviewed in Chitwood et al., 2007). Furthermore, instead of epistasis, *rgd2 lbl1* double mutants display synergistic shootless phenotypes, which suggest that RGD2 and/or LBL1 perform nonoverlapping functions outside of ta-siARF biogenesis (Henderson et al., 2006). Similar to *lbl1* and the rice *ago7* mutant *sho2*, *rgd2-R* mutant shoot apices exhibit ectopic overaccumulation of miR166 in adaxial leaf domains, although *lbl1* also accumulates ectopic miR166 at the base of the SAM (Nagasaki et al., 2007; Nogueira et al., 2007; Figures 5B and 6B). As such, our findings are consistent with suggested models wherein ta-siARF negatively regulates the expression of the abaxial-determinant miR166 (Figure 1; Nagasaki et al., 2007; Nogueira et al., 2007, 2009). Thus, despite the fact that *rgd2* and *lbl1* mutants both overexpress *arf3a* and ectopically accumulate miR166, they condition disparate leaf phenotypes. These data, when considered in light of the syner-

gistic *rgd2 lbl1* double mutant phenotype, suggest that LBL1 performs additional functions contributing to maize leaf polarity, outside of the ta-siARF biogenesis pathway.

In addition to its role during ta-siARF biogenesis, *Arabidopsis* SGS3 is also required for production of AGO1 siRNAs that downregulate the accumulation of AGO1 mRNA in conjunction with miR168 (Mallory and Vaucheret, 2009). Unlike AGO7, AGO1 binds numerous miRNA species, including miR166. Our data demonstrate that *lbl1-ref* mutants overaccumulate transcripts of a putative paralog of *ago1*, whereas *rgd2-R* mutants do not (Figure 4C). Recent studies have shown that a maize *ago1*-like transcript accumulates in a gradient within leaf primordia, with higher accumulation in adaxial domains (Brooks et al., 2009). Intriguingly, miR166 accumulates ectopically in adaxial leaf domains of *lbl1* mutants, in a pattern that overlaps with *ago1* accumulation. We propose that upregulation of *ago1* in *lbl1* mutants (Figure 4C), in conjunction with the ectopic overaccumulation of miR166, may result in enhanced posttranscriptional degradation of adaxial identity factor *hd-zipIII* genes. This increase in miR166 activity may explain why *lbl1* mutants lose adaxial identity while *rgd2* mutants do not. Furthermore, *Arabidopsis* SGS3 functions during viral defense and in additional siRNA pathways besides ta-siRNA biosynthesis (Mourrain et al., 2000; Peragine et al., 2004; Borsani et al., 2005). We propose a revised model (Figure 7) wherein additional functions of LBL1 outside of ta-siARF biogenesis contribute to the abaxialized phenotypes observed in *lbl1* mutants and to the synergistic, shootless phenotype seen in *rgd2 lbl1* double mutants (Henderson et al., 2006).

The interplay of several small RNAs is critical to the dorsiventral patterning of maize leaves (Chitwood et al., 2007; reviewed in Kidner and Timmermans, 2007). Future studies probing the mechanisms of miR390 polarization and its RGD2-mediated localization in the shoot apex will enhance our understanding of the role of regulatory RNAs during leaf development. In addition, identification and analyses of *arf3a* mutants in maize may help decipher the convergent and divergent mechanisms by which ta-siARF regulates the development of monocot and eudicot shoots.

METHODS

Plant Materials

The *rgd2-R* mutation arose in a *Mutator* transposon line (Henderson et al., 2005) and was introgressed into the maize (*Zea mays*) inbred Mo17 genetic background for at least four to five generations to generate the mapping population used in this study. Primers for novel molecular markers developed during this study are listed in Supplemental Table 1 online.

EMS-mutagenized Mo17 pollen was crossed to *rgd2-R* heterozygous individuals to obtain additional mutant alleles of *rgd2* as described (Neuffer, 1993). One EMS allele, *rgd2-e1*, was identified in a noncomplementation screen of ~6200 F1 plants. However, the *rgd2-R/rgd2-e1* heterozygous plant was seedling lethal, and the lesion was not recoverable for further genetic analyses. An additional mutant allele of *rgd2*, *rgd2-e2*, was obtained via screens of ~3000 M2 EMS-mutagenized families in the B73 inbred background. An M2 family segregated a filamentous leaf phenotype and was mapped to bin 1.04 using bulk segregant analyses. The *rgd2-Ds1* allele was identified in a large-scale transposon mutagenesis program using the transposons *Activator* and *Dissociation* (Ahern

et al., 2009). Analyses of the *lhl1-rgd1* allele were performed in the Mo17 genetic background.

In Situ Hybridizations

Samples from 14-d-old seedlings were fixed, processed, sectioned, and hybridized to gene-specific probes as described (Jackson, 1991) with modifications as described (Juarez et al., 2004). Double-digoxigenin (DIG)-labeled LNA probes complementary to miR390, miR166, and ta-siARF were purchased from Exiqon. Five picomoles of LNA probe were used per slide; hybridizations were performed at 50°C, and washes were performed at 55°C. The *rgd2* and *tas3a* probes (see Supplemental Table 1 online) were DIG labeled (Roche) according to the manufacturer's instructions. All samples were imaged on a Zeiss Axio Imager Z1m microscope using a 5-megapixel Zeiss AxioCam MRc5 and AxioVision Release 4.6 software.

Small RNA Gel Blot Hybridization

miRNA gel blots were performed as described (Allen et al., 2004). Fifteen hand-dissected apices (shoot apex plus six leaf primordia) were pooled for each wild-type and *rgd2-R* mutant sample; RNA was extracted using the Trizol lysis method and prepared for RNA gel blot transfer as described (Fu et al., 2002). Approximately 20 µg of total RNA was loaded per lane. Twenty-one base pair oligonucleotide probes complementary to miR390 and miR166 were end labeled with ³²P. Double-DIG-labeled LNA ta-siARF probes were as described above. Hybridizations and washes were performed at 42°C.

qRT-PCR

SAM or leaf primordia (P1-P4) tissue was harvested by LM, and cDNA was synthesized from amplified RNA as described by Zhang et al. (2007). Gene-specific primers were designed (see Supplemental Table 1 online) for use with SYBR-Green (Quanta) in qRT-PCR as described (Zhang et al., 2007). Three biological replicates were examined, and samples were normalized to *beta-6 tubulin* or *ubiquitin* expression as described using Bio-Rad iQ5 Version 1.0 software (Livak and Schmittgen, 2001; Zhang et al., 2007).

Accession Numbers

Sequence data can be found in the GenBank data library under the following accession numbers: BAC c0230J20 (AC206196), *rgd2* (GQ918490), *Zm ago1* (AY110984), *tubulin* (L10633), and *ubiquitin* (S94464).

Supplemental Data

The following materials are available in the online version of this article.

Supplemental Figure 1. DNA Gel Blot Analysis of Maize *ago7*

Supplemental Figure 2. Amino Acid Alignment of RGD2, AGO7, and SHO2.

Supplemental Figure 3. Additional in Situ Hybridization Analyses of miR390 Accumulation in *rgd2-R* Mutant Apices.

Supplemental Table 1. Primers Used in This Study.

ACKNOWLEDGMENTS

We thank Marja Timmermans and Dan Chitwood for assistance with small RNA in situ hybridizations; Xiaolan Zhang donated LM SAM cDNA,

and Dave Henderson provided helpful discussions of the data. We thank Gary Muehlbauer for identification of *rgd2* mutant alleles and Erik Vollbrecht, Tom Brutnell, and Kevin Ahern for identifying the *rgd2-Ds1* allele. Scott Tingey and Amanda Jones provided physical mapping information that expedited the positional cloning of *rgd2*, and Taiowa Montgomery offered technical advice on small RNA gel blot hybridizations. This work was supported by the National Science Foundation (Grants IOS-0649810 and IOS-0820610 to M.J.S.).

Received October 8, 2009; revised April 9, 2010; accepted April 22, 2010; published May 7, 2010.

REFERENCES

- Adenot, X., Elmayer, T., Laressergues, D., Boutet, S., Bouche, N., Gascioli, V., and Vaucheret, H. (2006). DRB4-dependant *TAS3* *trans*-acting siRNAs control leaf morphology through AGO7. *Curr. Biol.* **18**: 758–762.
- Ahern, K.R., Deewatthanawong, P., Schares, J., Muszynski, M., Weeks, R., Vollbrecht, E., Duvick, J., Brendel, V.P., and Brutnell, T.P. (2009). Regional mutagenesis using *Dissociation* in maize. *Methods* **49**: 248–254.
- Allen, E., Xie, Z., Gustafson, A.M., and Carrington, J.C. (2005). MicroRNAs-directed phasing during *trans*-acting siRNA biogenesis in plants. *Cell* **121**: 207–221.
- Allen, E., Xie, Z., Gustafson, A.M., Sung, G.H., Spatafora, J.W., and Carrington, J.C. (2004). Evolution of microRNA genes by inverted duplication of target gene sequences in *Arabidopsis thaliana*. *Nat. Genet.* **36**: 1282–1290.
- Alvarez, J.P., Pekker, I., Goldshmidt, A., Blum, E., Amsellem, Z., and Eshed, Y. (2006). Endogenous and synthetic microRNAs stimulate simultaneous, efficient, and localized regulation of multiple targets in diverse species. *Plant Cell* **18**: 1134–1151.
- Borsani, O., Zhu, J., Verslues, P.E., Sunkar, R., and Zhu, J.K. (2005). Endogenous siRNAs derived from a pair of natural *cis*-antisense transcripts regulate salt tolerance in *Arabidopsis*. *Cell* **123**: 1279–1291.
- Brooks III, L.B., et al. (2009). Microdissection of shoot meristem functional domains. *PLoS Genet.* **5**: e1000476.
- Chitwood D.H., Guo M., Nogueira F.T., and Timmermans M.C. (2007). Establishing leaf polarity: the role of small RNAs and positional signals in the shoot apex. *Development* **134**: 813–823.
- Chitwood, D.H., Nogueira, F.T.S., Howell, M.D., Montgomery, T.A., Carrington, J.C., and Timmermans, M.C.P. (2009). Pattern formation via small RNA mobility. *Genes Dev.* **23**: 549–554.
- Eshed, Y., Izhaki, A., Baum, S.F., Floyd, S.K., and Bowman, J.L. (2004). Asymmetric leaf development and blade expansion in *Arabidopsis* are mediated by KANADI and YABBY activities. *Development* **131**: 2997–3006.
- Fagard, M., Boutet, S., Morel, J.B., Bellini, C., and Vaucheret, H. (2000). AGO1, QDE-2, and RDE-1 are related proteins required for post-transcriptional gene silencing in plants, quelling in fungi, and RNA interference in animals. *Proc. Natl. Acad. Sci. USA* **97**: 11650–11654.
- Fahlgren, N., Montgomery, T., Howell, M., Allen, E., Dvorak, S., Alexander, A., and Carrington, J. (2006). Regulation of *AUXIN RESPONSE FACTOR3* by *TAS3* ta-siRNA affects developmental timing and patterning in *Arabidopsis*. *Curr. Biol.* **16**: 939–944.
- Fu, S., Meeley, R., and Scanlon, M.J. (2002). *Empty pericarp2* encodes a negative regulator of the heat shock response and is required for maize embryogenesis. *Plant Cell* **14**: 3119–3132.

- Garcia, D., Collier, S.A., Byrne, M.E., and Martienssen, R.A. (2006). Specification of leaf polarity in *Arabidopsis* via the *trans*-acting siRNA pathway. *Curr. Biol.* **16**: 933–938.
- Henderson, D.C., Muehlbauer, G.J., and Scanlon, M.J. (2005). Radial leaves of the maize mutant *ragged seedling2* retain dorsiventral anatomy. *Dev. Biol.* **282**: 455–466.
- Henderson, D.C., Zhang, X., Brooks, L., and Scanlon, M.J. (2006). RAGGED SEEDLING2 is required for normal expression of KANADI2 and REVOLUTA homologues in the maize shoot apex. *Genesis* **44**: 372–382.
- Hunter, C., Sun, H., and Poethig, S.R. (2003). The *Arabidopsis* heterochronic gene *ZIPPY* is an *ARGONAUTE* family member. *Curr. Biol.* **13**: 1734–1739.
- Hunter, C., Willmann, M.R., Wu, G., Yoshikawa, M., de la Luz Gutierrez-Nava, M., and Poethig, S.R. (2006). *Trans*-acting siRNA-mediated repression of *ETTIN* and *ARF4* regulates heteroblasty in *Arabidopsis*. *Development* **133**: 2973–2981.
- Husbands, A.Y., Chitwood, D.H., Plavskin, Y., and Timmermans, M.C. (2009). Signals and prepatterns: new insights into organ polarity in plants. *Genes Dev.* **23**: 1986–1997.
- Hutvagner, G., and Simard, M.J. (2008). Argonaute proteins: Key players in RNA silencing. *Nat. Rev. Mol. Cell Biol.* **9**: 22–32.
- Itoh, J., Sato, Y., and Nagato, Y. (2008). The SHOOT ORGANIZATION2 gene coordinates leaf domain development along the central-marginal axis in rice. *Plant Cell Physiol.* **49**: 1226–1236.
- Jackson, D. (1991). In situ hybridization in plants. In *Molecular Plant Pathology: A Practical Approach*, D.J. Bowles, S.J. Gurr, and M. McPherson, eds (Oxford, UK: Oxford University Press), pp. 163–174.
- Juarez, M.T., Kui, J., Thomas, J., Heller, B., and Timmermans, M.C.P. (2004). MicroRNA-mediated repression of *rolled leaf1* specifies maize leaf polarity. *Nature* **428**: 84–88.
- Koch, A.J., and Meinhardt, H. (1994). Biological pattern-formation – From basic mechanisms to complex structures. *Rev. Mod. Phys.* **66**: 1481–1507.
- Kidner, C.A., and Martienssen, R.A. (2004). Spatially restricted microRNA directs leaf polarity through *ARGONAUTE1*. *Nature* **428**: 81–84.
- Kidner, C.A., and Timmermans, M.C.P. (2007). Mixing and matching pathways in leaf polarity. *Curr. Opin. Plant Biol.* **10**: 13–20.
- Lanet, E., Delannoy, E., Sormani, R., Floris, M., Brodersen, P., Crete, P., Voinnet, O., and Robaglia, C. (2009). Biochemical evidence for translational repression by *Arabidopsis* microRNAs. *Plant Cell* **21**: 1762–1768.
- Lingel, A., Simon, B., Izaurralde, E., and Sattler, M. (2004). Nucleic acid 3'-end recognition by the Argonaute2 PAZ domain. *Nat. Struct. Mol. Biol.* **11**: 576–577.
- Livak, K.J., and Schmittgen, T.D. (2001). Analysis of relative gene expression data using real-time quantitative PCR and the $2^{-\Delta\Delta C_T}$ (Delta Delta C(T)). *Methods* **25**: 402–408.
- Lu, C., Kulkarni, K., Souret, F.F., MuthuValliappan, R., Tej, S.S., Poethig, R.S., Henderson, I.R., Jacobsen, S.E., Wang, W., Green, P.J., and Meyers, B.C. (2006). MicroRNAs and other small RNAs enriched in the *Arabidopsis* RNA-dependent RNA polymerase-2 mutant. *Genome Res.* **16**: 1276–1288.
- Ma, J.B., Ye, K., and Patel, D.J. (2004). Structural basis for overhang-specific small interfering RNA recognition by the PAZ domain. *Nature* **429**: 318–322.
- Mallory, A.C., and Vaucheret, H. (2009). ARGONAUTE1 homeostasis invokes the coordinate action of the microRNA and siRNA pathways. *EMBO Rep.* **10**: 521–526.
- McConnell, J.R., Emery, J., Eshed, Y., Bao, N., Bowman, J., and Barton, M.K. (2001). Role of PHABULOSA and PHAVOLUTA in determining radial patterning in shoots. *Nature* **411**: 709–713.
- Montgomery, T.A., Howell, M.D., Cuperus, J.T., Li, D., Hansen, J.E., Alexander, A.L., Chapman, E.J., Fahlgren, N., Allen, E., and Carrington, J.C. (2008). Specificity of ARGONAUTE7-miR390 interaction and dual functionality in TAS3 *trans*-acting siRNA formation. *Cell* **133**: 128–141.
- Mourrain, P., et al. (2000). *Arabidopsis* SGS2 and SGS3 genes are required for posttranscriptional gene silencing and natural virus resistance. *Cell* **101**: 533–542.
- Nagasaki, H., Itoh, J., Hayashi, K., Hibara, K., Satoh-Nagasawa, N., Nosaka, M., Mukouhata, M., Ashikari, M., Kitano, H., Matsuoka, M., Nagato, Y., and Sato, Y. (2007). The small interfering RNA production pathway is required for shoot meristem initiation in rice. *Proc. Natl. Acad. Sci. USA* **104**: 14867–14871.
- Neuffer, M.G. (1993). Mutagenesis. In *The Maize Handbook*, M. Freeling and V. Walbot, eds (New York: Springer), pp. 212–219.
- Nogueira, F.T., Chitwood, D.H., Madi, S., Ohtsu, K., Schnable, P.S., Scanlon, M.J., and Timmermans, M.C. (2009). Regulation of small RNA accumulation in the maize shoot apex. *PLoS Genet.* **5**: e1000320.
- Nogueira, F.T., Madi, S., Chitwood, D.H., Juarez, M.T., and Timmermans, M.C. (2007). Two small regulatory RNAs establish opposing fates of a developmental axis. *Genes Dev.* **21**: 750–755.
- Pekker, I., Alvarez, J., and Eshed, Y. (2005). AUXIN RESPONSE FACTORS mediate *Arabidopsis* organ asymmetry via modulation of KANADI activity. *Plant Cell* **17**: 2899–2910.
- Peragine, A., Yoshikawa, M., Wu, G., Albrecht, H.L., and Poethig, R.S. (2004). SGS3 and SGS2/SDE1/RDR6 are required for juvenile development and the production of *trans*-acting siRNAs in *Arabidopsis*. *Genes Dev.* **18**: 2368–2379.
- Poethig, R.S. (1984). Cellular parameters of leaf morphogenesis in maize and tobacco. In *Contemporary Problems of Plant Anatomy*, R.A. White and W.C. Dickinson, eds (New York: Academic Press), pp. 235–238.
- Reinhart, B.J., Weinstein, E.G., Rhoades, M.W., Bartel, B., and Bartel, D.P. (2002). MicroRNAs in plants. *Genes Dev.* **16**: 1616–1626.
- Schwab, R., Ossowski, S., Riester, M., Warthmann, N., and Weigel, D. (2006). Highly specific gene silencing by artificial microRNAs in *Arabidopsis*. *Plant Cell* **18**: 1121–1133.
- Talbert, L.E., Patterson, G.I., and Chandler, V.L. (1989). *Mu* transposable elements are structurally diverse and distributed throughout the genus *Zea*. *J. Mol. Evol.* **29**: 28–39.
- Timmermans, M.C., Schultes, N.P., Jankovsky, J.P., and Nelson, T. (1998). Leafbladeless1 is required for dorsoventrality of lateral organs in maize. *Development* **125**: 2813–2823.
- Tretter, E.M., Alvarez, J.P., Eshed, Y., and Bowman, J.L. (2008). Activity range of *Arabidopsis* small RNAs derived from different biogenesis pathways. *Plant Physiol.* **147**: 58–62.
- Vaucheret, H. (2008). Plant ARGONAUTES. *Trends Plant Sci.* **13**: 350–358.
- Waites, R., and Hudson, A. (1995). *phantastica*: A gene required for dorsoventrality of leaves in *Antirrhinum majus*. *Development* **121**: 2143–2154.
- Yoshikawa, M., Peragine, A., Park, M.Y., and Poethig, R.S. (2005). A pathway for the biogenesis of *trans*-acting siRNAs in *Arabidopsis*. *Genes Dev.* **19**: 2164–2175.
- Zhang, X., Madi, S., Borsuk, L., Nettleton, D., Elshire, R.J., Buckner, B., Janick-Buckner, D., Beck, J., Timmermans, M., Schnable, P.S., and Scanlon, M.J. (2007). Laser microdissection of narrow sheath mutant maize uncovers novel gene expression in the shoot apical meristem. *PLoS Genet.* **3**: e101.
- Zhong, R., and Ye, Z.H. (2004). Amphivasal vascular bundle1, a gain-of-function mutation of the IFL1/REV gene, is associated with alterations in the polarity of leaves, stems and carpels. *Plant Cell Physiol.* **45**: 369–385.